IOPscience iopscience.iop.org

Home Search Collections Journals About Contact us My IOPscience

Electron scattering in a polarization superlattice

This article has been downloaded from IOPscience. Please scroll down to see the full text article.

2002 J. Phys.: Condens. Matter 14 3469

(http://iopscience.iop.org/0953-8984/14/13/306)

View the table of contents for this issue, or go to the journal homepage for more

Download details:
IP Address: 171.66.16.104
The article was downloaded on 18/05/2010 at 06:23

Please note that terms and conditions apply.

INSTITUTE OF PHYSICS PUBLISHING JOURNAL OF PHYSICS: CONDENSED MATTER

J. Phys.: Condens. Matter **14** (2002) 3469–3478 PII: S0953-8984(02)27966-7

Electron scattering in a polarization superlattice

B K Ridley

Department of Electronic Systems Engineering, University of Essex, Colchester, CO4 3SQ, UK

Received 16 August 2001, in final form 14 September 2001
Published 22 March 2002
Online at stacks.iop.org/JPhysCM/14/3469

Abstract

A superlattice composed of materials exhibiting spontaneous electrical polarization has strong electric fields in both wells and barriers. Electrons in the wells are confined in deep triangular potentials whereas polar-optical phonons are confined in square wells. The electron–phonon interaction therefore presents novel features, and these are explored here in the system $Al_{1-x}In_xN/GaN$ assumed to be lattice-matched. The dielectric-continuum model is used to calculate bulk alloy and interface mode properties, and threshold scattering rates are estimated. The reduced role of phonon symmetry is pointed out.

1. Introduction

Spontaneous polarization in nitride structures gives rise to large static electric fields that confine electrons in approximately triangular quantum wells. On the other hand optical phonons in a nitride superlattice have the usual confinement and interface properties of a square quantum well. The electron–phonon interaction in a situation where the quantum confinements of electrons and phonons are different spatially has not received much attention hitherto. In this paper we address the problem of describing the scattering of electrons confined in a triangular quantum well by their interaction with polar-optical phonons confined in a square quantum well.

As an example of a polarization superlattice we consider the system $Al_{1-x}In_xN/GaN$ for the lattice-matched condition $x \approx 0.17$. The polarization then arises purely from spontaneous polarization, with no piezoelectric component. The calculation then proceeds as follows. A periodic electric-field profile is established for the superlattice using estimates of the spontaneous polarization in the AlInN barrier and in the GaN well. Airy function solutions for the triangular well are then used to define the subband energies, and Fang–Howard wavefunctions are used to approximate the Airy functions and to provide phonon overlap integrals. The allowed optical-phonon frequencies in the alloy and in the binary are established using standard dielectric-continuum (DC) theory. Explicit scattering rates are obtained for the intra-subband transition from the phonon-energy threshold and from the bottom of the second subband in a 100 Å well. A comparison is made with the results that arise from the assumption

 © 2002 IOP Publishing Ltd Printed in the UK

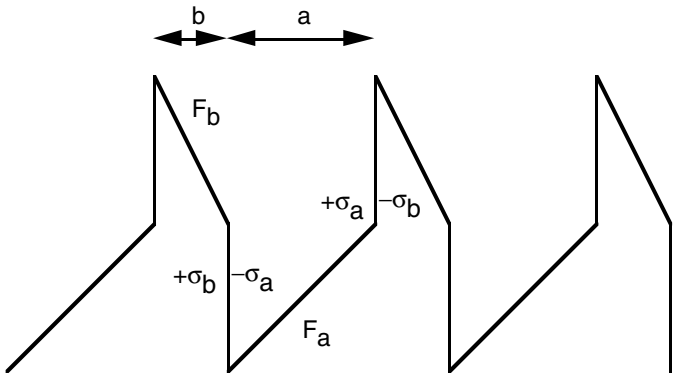

Figure 1. A polarization superlattice.

that the phonons are bulk-like. Finally, a better approximation to the ground-state Airy function is given and the results are compared with those using Fang–Howard wavefunctions.

2. The polarization superlattice

A polarization superlattice is depicted in figure 1. Periodicity implies that

$$\varepsilon_b F_b - \varepsilon_a F_a = \sigma_a - \sigma_b \qquad -bF_b - aF_a = 0 \tag{1}$$

where $\varepsilon_{a,b}$ are the permittivities of the well and barrier materials, $F_{a,b}$ are the electric fields, $\sigma_{a,b}$ are the spontaneous polarizations with $\sigma_b > \sigma_a$ and a, b the dimensions of the well and barrier, respectively. The equations follow from Gauss's theorem and the condition of zero-voltage drop across a superlattice element. It is assumed that the electron population in the well is insignificant, implying the existence of appropriate boundary conditions at the superlattice extremes. Solving equation (1) for the field in the well gives

$$F_a = \frac{\sigma_b - \sigma_a}{\varepsilon_a \left(1 + \frac{\varepsilon_b a}{\varepsilon_a b}\right)}. \tag{2}$$

3. Electrons

Taking the discontinuity of the conduction-band edge to be about 66% of the difference of energy gaps between $Al_{0.83}In_{0.17}N$ and GaN leads to $E_c \approx 1.4$ eV. This is large enough for us to assume that any penetration of the electron wavefunction into the barrier is negligible. Strictly, the solution for the wavefunction will be a linear combination of the independent solutions of the Airy equation that matches a similar solution in the barriers, but given the large band-edge discontinuity and limiting attention to wide wells (given the large polarization fields this means limiting attention to well widths greater than 50 Å) the wavefunction can be taken to a sufficient approximation to be a simple Airy function.

The subband energies in the triangular well are then taken to be adequately expressed by

$$E_n = \left(\frac{\hbar^2}{2m^*}\right)^{1/3} \left(\frac{3\pi e F}{2}\left(n + \frac{3}{4}\right)\right)^{2/3} \tag{3}$$

with the solution of the Schrödinger equation given by the Airy function

$$\Psi_n(z) = \mathrm{Ai}\left(\left(\frac{2m*}{\hbar^2 e^2 F^2}\right)^{1/3}(eFz - E_n)\right). \tag{4}$$

When extreme accuracy is not required it is analytically convenient to replace the Airy function with simpler expressions. We will use the Fang–Howard formulae [1, 2]

$$\Psi_1(z) = \left(\frac{b^3}{2}\right)^{1/2} z\mathrm{e}^{-bz/2} \qquad \Psi_2(z) = \left(\frac{3b^3}{2}\right)^{1/2} z\left(1 - \frac{bz}{3}\right)\mathrm{e}^{-bz/2}. \tag{5}$$

and choose b (not to be confused with barrier width) to give the correct energy for E_1. This fomulation, which emphasizes the properties of the triangular well, will be valid only for sufficiently wide wells. We also assume that the communication between wells is negligible, which is equivalent to assuming that the superlattice is a series of single quantum wells. This will be true provided, once again, that the well width is not too small.

4. Phonons

The two-mode character of the alloy is quantified using the assumption that the dielectric function can be expressed as the sum of the polarizabilities of the two binaries AlN and InN [3] as was done for AlGaN [4]. These alloy modes have frequencies that lie in the vicinity of the LO and TO frequencies of GaN, which might suggest that they may propagate through the superlattice. However, the discrepancy in the mass factors of the alloy and GaN is the crucial factor [5] and in fact the alloy modes will be substantially confined to the alloy. We are assuming that the discontinuity in the conduction-band edges is large enough to make any electron penetration negligible and so we can forget about the role of bulk alloy modes with regard to scattering.

But we cannot forget about the associated interface modes. All told there will be three such modes and each will contribute to the scattering. Strictly speaking, there will be modes of mixed character, interface and bulk. This hybridization is required in order to satisfy both electromagnetic and mechanical boundary conditions [6, 7], neglect of which gives rise to wrong mode patterns as revealed by Raman scattering. However, as far as overall scattering rates are concerned it turns out that the set of modes obtained if the mechanical boundary conditions are ignored, i.e. using the DC model, describes the scattering rate adequately [8]. Because of the comparative simplicity of the DC model we will use it to calculate scattering rates. Satisfying the electrical boundary conditions at each interface, but ignoring the mechanical boundary conditions, leads to the dispersion relation for interface modes [9]:

$$\cos k_z(a+b) - \frac{1+r^2}{2r}\sinh qa\,\sinh qb - \cosh qa\,\cosh qb = 0 \tag{6}$$

where k_z ($0 \leqslant k_z(a+b) \leqslant \pi$) is the wave vector along the superlattice axis, q is the in-plane wave vector and $r = \varepsilon_a(\omega)/\varepsilon_b(\omega)$. Here

$$\varepsilon_b(\omega) = \varepsilon_{\infty b}\frac{\left(\omega^2 - \omega_+^2\right)\left(\omega^2 - \omega_-^2\right)}{\left(\omega^2 - \omega_{T1}^2\right)\left(\omega^2 - \omega_{T2}^2\right)} \qquad \varepsilon_a(\omega) = \varepsilon_{\infty a}\frac{\left(\omega^2 - \omega_{La}^2\right)}{\left(\omega^2 - \omega_{Ta}^2\right)} \tag{7}$$

where $\varepsilon_{\infty b}$ is the high-frequency permittivity of the alloy virtual crystal, $\varepsilon_{\infty a}$ is the same for the well material, $\omega_\pm$ are the angular frequencies of the alloy modes, $\omega_{T1,T2}$ are the TO frequencies of the binaries in the alloy and $\omega_{La,Ta}$ are the LO and TO frequencies of the well material. Equations (6) and (7) predict three interface bands.

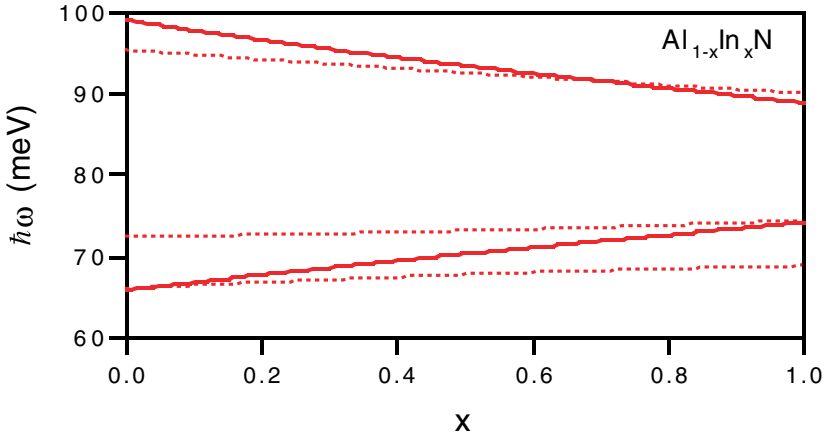

Figure 2. Bulk alloy mode frequencies (solid lines). Interface mode frequencies (dashed lines) according to equation (8).

Table 1. Parameters of alloys.

	AlN	InN	GaN
$\hbar\omega$T (meV)	74.3	65.9	70.7
$\hbar\omega$L (meV)	99.2	89.0	91.2
$\varepsilon/\varepsilon_0$	4.77	8.4	5.35
$\varepsilon_s/\varepsilon_0$	8.5	15.3	8.9
$P_{\rm sp}$ (cm^{-2})	−0.081	−0.032	−0.029

The general situation is quite complicated since the mode patterns for a given interface band in the well depend upon the superlattice wave vector and are only simply symmetric or antisymmetric for $k_z(a+b) = 0\,\text{or}\,\pi$. However, the situation simplifies considerably when qa, qb and $q(a-b)$ (or $q(b-a)$) are large enough, a condition that is easily satisfied in the nitride systems as a consequence of the large phonon energies (leading to large q) for wells and barriers that are not too thin.

When this is the case the dispersion relation reduces to

$$\varepsilon_a(\omega) + \varepsilon_b(\omega) = 1 \tag{8}$$

and the mode patterns can be shown to be independent of the superlattice wave vector, being either sinh-like or cosh-like. The frequencies of the two modes in the alloy and of the interface modes are shown in figure 2. The parameters used are those in the table 1.

The DC theory also gives the Fröhlich coupling strengths of the modes. The ones of interest are, of course, the interface modes and the confined well modes since these are the only modes that interact with electrons in the triangular well. (As mentioned earlier, it is assumed that the electron wavefunction does not penetrate the barrier.) Of the interface modes only the highest-frequency one has non-negligible coupling strength. The others, being more TO-like, have small coupling strengths and their influence can be neglected. Explicit expressions in terms of the rate W_0, where

$$W_0 = \frac{e^2}{4\pi\hbar}\left(\frac{2m^*\omega}{\hbar}\right)^{1/2}\frac{1}{\varepsilon^*} \tag{9}$$

are for the confined well modes

$$\frac{1}{\varepsilon^*} = \frac{1}{\varepsilon_{\infty a}} - \frac{1}{\varepsilon_{sa}} \tag{10}$$

where ε_{sa} is the static permittivity; and for the interface modes

$$\begin{aligned}
\frac{1}{\varepsilon^*} &= \frac{1}{\beta_a + \beta_b} \\
\beta_a &= \varepsilon_{\infty a}\omega^2 \frac{\omega_{La}^2 - \omega_{Ta}^2}{\omega^2 - \omega_{Ta}^2} \\
\beta_b &= \varepsilon_{\infty b}\omega^2 \frac{X_{1b}\left(\omega^2 - \omega_{T2}^2\right) + X_{2b}\left(\omega^2 - \omega_{T1}^2\right)}{\left(\omega^2 - \omega_{T1}^2\right)^2\left(\omega^2 - \omega_{T2}^2\right)^2} \\
X_{1b} &= \frac{\left(\omega_+^2 - \omega_{T1}^2\right)\left(\omega_+^2 - \omega_{T2}^2\right)}{\left(\omega_+^2 - \omega_-^2\right)} \\
X_{2b} &= \frac{\left(\omega_-^2 - \omega_{T1}^2\right)\left(\omega_-^2 - \omega_{T2}^2\right)}{\left(\omega_-^2 - \omega_+^2\right)}.
\end{aligned} \tag{11}$$

5. Scattering rates

Scattering rates are computed for two special cases, namely, intra-subband scattering from an energy equal to the phonon energy, and inter-subband scattering from the bottom of the second subband into the first. We refer to these as threshold rates. The threshold scattering rate from subband i to subband j for a given mode is given by

$$W_{ij} = W_0 2\pi^2 \left(\frac{\hbar\omega}{E_0}\right)^{1/2} \frac{|G_{ij}|^2}{(Qa)^2}. \tag{12}$$

Here W_0 is the rate defined in equation (9), $E_0 = \hbar^2\pi^2/2m^*a^2$, G_{ij} is the overlap integral and Q is a normalizing factor. The confined well modes have envelope functions for their scalar potential given by $\sin(n\pi z/a)$, where $n = 1, 2, 3$, etc and

$$G_{ij} = \int_0^\infty \psi_j \, \sin(n\pi z/a)\psi_i \, \mathrm{d}z \qquad Qa = \sqrt{(q^2a^2 + (n\pi)^2)}. \tag{13}$$

The active interface mode has a symmetric profile—$\cosh(q(z - a/2))$—and an antisymmetric profile—$\sinh(q(z - a/2))$, so

$$G_{ij} = \int_0^\infty \psi_j \begin{cases} \cosh(q(z - a/2)) \\ \sinh(q(z - a/2)) \end{cases} \psi_i \, \mathrm{d}z \qquad (Qa)^2 = 4qa \begin{cases} \cosh^2(qa/2) \\ \sinh^2(qa/2). \end{cases} \tag{14}$$

The expression for Qa is the normalizing factor assuming that the interface modes are essentially barrier modes. In these expressions q is the in-plane phonon wave vector satisfying momentum conservation. The general expressions for the overlap integrals are given in the appendix.

The in-plane wave vector q is determined in the first case by the phonon energy and in the second case by the subband separation, assumed to be greater than the phonon energy. The parameters are shown in table 1. The composition dependence of the alloy was taken to be linearly dependent on x and bowing parameters were ignored. The electron effective mass was taken to be 0.2 m_0.

Figure 3 shows the form factors $|G_{ij}|^2/Q^2$ for the first eight GaN confined LO modes in a 100 Å well containing an electron-confining triangular well in the $Al_{0.83}In_{0.17}N$/GaN

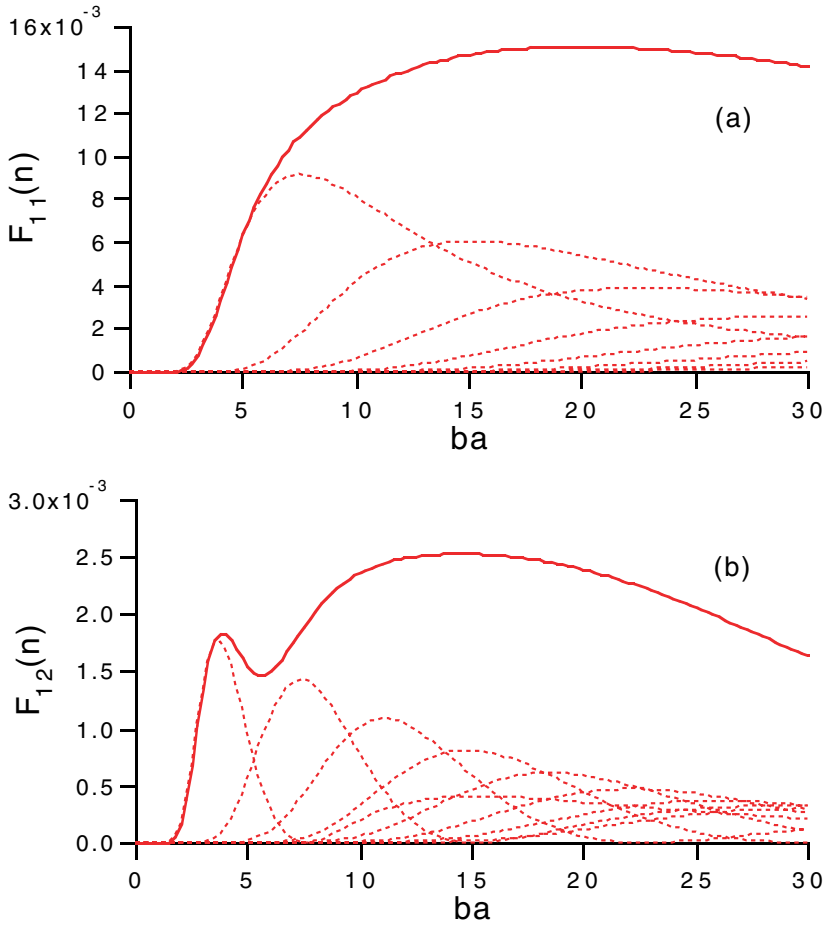

Figure 3. Form factors for the first eight confined GaN modes at emission threshold: (a) intra-subband and (b) inter-subband.

superlattice in which $ba = 0.18$ and the inter-subband separation was taken to be 0.31 eV (barrier width 50 Å). In the conventional case, where the electron is confined in the same square well as the phonons, symmetry would rule out contributions from even number (antisymmetrical) modes for the intra-subband transition and odd number (symmetrical) modes for the inter-subband transition with, in both cases, emphasis on the lowest-order mode. In the case of the triangular well symmetry does not play such a large role and higher-order modes contribute relatively more. The smaller part that symmetry has to play is also shown for interface modes (figure 4). Only when *ba* is relatively small, so that the electron wavefunction is more evenly spread across the square well, does symmetry matter.

Adding the contributions from the confined modes and from both the symmetric and antisymmetric interface modes we obtain for the intra-subband threshold emission rate 9.07×10^{13} s^{-1} and for the inter-subband 1.32×10^{13} s^{-1}. It is interesting to compare these results with those obtained by assuming that the phonon modes are GaN bulk unconfined modes. The rates of scattering by bulk modes are, respectively, 1.04×10^{14} s^{-1} and 1.58×10^{13} s^{-1}.

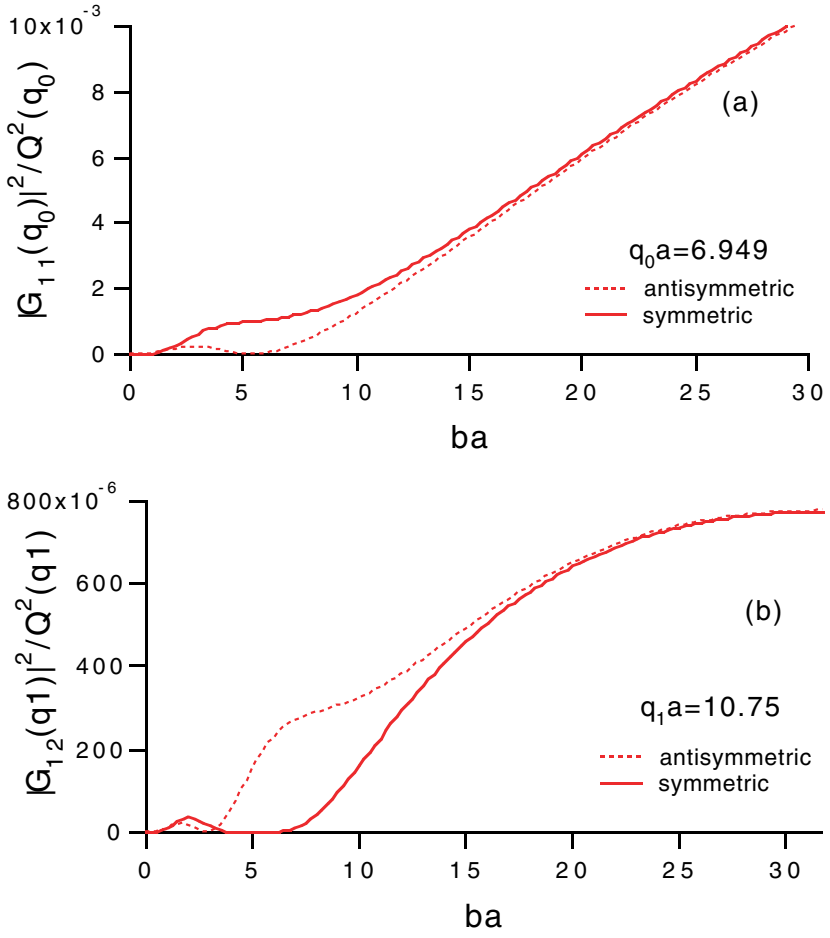

Figure 4. Form factors for the active interface mode at emission threshold: (a) intra-subband and (b) inter-subband.

6. Discussion

The similarity of these rates obtained from confined and unconfined well modes is a common result. It is associated with an approximate sum-rule affecting any complete set of modes [10–12]. The sum-rule would be precise were the Fröhlich coupling strength to be the same for every mode. For confined and bulk modes the coupling strength is dependent on frequency and, therefore, given the weak dispersion of long-wavelength optical modes, it is nearly the same for each mode. In the system considered, the interface modes have closely similar coupling strengths, so the condition is fulfilled for the sum-rule to work to a good approximation. This has allowed us, for simplicity, to follow standard usage and to use the DC model (which neglects mechanical boundary conditions) to obtain the scattering rates.

For simplicity we have assumed that the subband energies of the electrons and their wavefunctions are those of a pure triangular well. The use of this assumption produces a tension when the triangular well is situated in a finite-width layer since the exponential tail of the wavefunction cannot stretch to infinity as assumed by the use of Airy functions and the

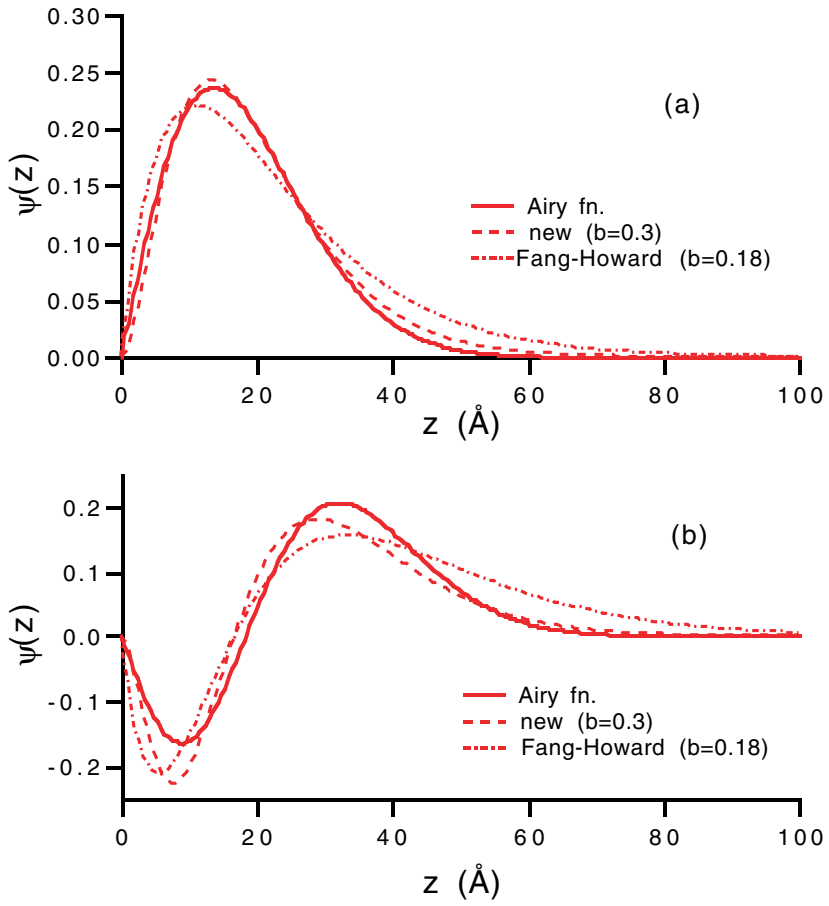

Figure 5. Comparison of wavefunction models: (a) ground state and (b) first excited state.

Fang–Howard approximations to them. However, this does not introduce major inaccuracies provided that the well is wide enough. The width of 100 Å chosen here satisfies this condition extremely well.

Given the adequacy of triangular-well wavefunctions it is pertinent to consider more accurate models than those of Fang and Howard to replace the Airy functions in order to allow relatively simple analytic results to be obtained. A better fit, at least to the ground-state wavefunction, is obtained by using the following:

$$\psi_1(z) = \left(\frac{b^5}{24}\right)^{1/2} z^2 \, \mathrm{e}^{-bz/2} \qquad \psi_1(z) = \left(\frac{b^5}{24}\right)^{1/2} z^2 \left(1 - \frac{bz}{5}\right) \mathrm{e}^{-bz/2}. \tag{15}$$

Figure 5 shows a comparison of this new model and the Fang–Howard model with Airy functions.

The form factors for the new model in the case of bulk modes are given in the appendix. The rates using the new model and relying on the sum-rule (i.e. using bulk modes) are 1.17×10^{14} s^{-1} and 1.58×10^{13} s^{-1} which may be compared to 1.04×10^{14} s^{-1} and 1.58×10^{13} s^{-1} obtained with Fang–Howard wavefunctions. This would indicate that the rates are not very sensitive to the difference between Fang–Howard wavefunctions and Airy wavefunctions.

Acknowledgments

The author has benefitted from discussions with Dr W Schaff at Cornell and would like to acknowledge support from the Office of Naval Research (grant no N000140110002) sponsored by Dr Colin Wood.

Appendix. Overlap integrals

1. Confined modes

$$G_{ij} = \int_0^a \psi_i \psi_j \, \sin(n\pi z/a)\, \mathrm{d}z. \tag{A.1}$$

Inserting Fang–Howard wavefunctions gives

$$\begin{aligned} G_{11}(n) &= \frac{(ba)^3 n\pi}{2}\left[\frac{2\{3(ba)^2-(n\pi)^2\}}{\{(ba)^2+(n\pi)^2\}^3} - \mathrm{e}^{-ba} f_{11}(b,n)\right] \\ G_{12}(n) &= \frac{(ba)^3 n\pi\sqrt{3}}{2}\left[\frac{2\{-(ba)^4+6(ban\pi)^2-(n\pi)^4\}}{3\{(ba)^2+(n\pi)^2\}^4} - \mathrm{e}^{-ba} f_{12}(b,n)\right]. \end{aligned} \tag{A.2}$$

The term involving the exponential in each of the expressions contributes little and in the spirit of our approximations can be ignored.

2. Interface modes

$$\begin{aligned} G_{ij}(q) &= \int_0^a \psi_i \psi_j \begin{Bmatrix} \cosh\{q(z-a/2)\} \\ \sinh\{q(z-a/2)\} \end{Bmatrix} \mathrm{d}z \\ G_{11}(q) &= \frac{(ba)^3}{2}\left[P_{11} + Q_{11} - \mathrm{e}^{-ba} f_{11}(b,q)\right] \end{aligned} \tag{A.3}$$

$$\begin{aligned} P_{11} &= \frac{2ba\{(ba)^2+3(qa)^2\}}{\{(ba)^2-(qa)^2\}^3} \begin{Bmatrix} +\cosh(qa/2) \\ -\sinh(qa/2) \end{Bmatrix} \\ Q_{11} &= \frac{2qa\{3(ba)^2-(qa)^2\}}{\{(ba)^2-(qa)^2\}^3} \begin{Bmatrix} -\sinh(qa/2) \\ +\cosh(qa/2) \end{Bmatrix} \end{aligned} \tag{A.4}$$

where the upper function refers to the symmetric and the lower to the antisymmetric interface mode. In this case the term involving the exponential cannot be neglected since it contains hyperbolic functions. Thus,

$$\begin{aligned} f_{11}(q) &= R_{11}\begin{Bmatrix} \cosh(qa/2) \\ \sinh(qa/2) \end{Bmatrix} + S_{11}\begin{Bmatrix} \sinh(qa/2) \\ \cosh(qa/2) \end{Bmatrix} \\ R_{11} &= \frac{ba}{(ba)^2-(qa)^2} + \frac{2\{(ba)^2+(qa)^2\}}{\{(ba)^2-(qa)^2\}^2} + \frac{2ba\{(ba)^2+3(qa)^2\}}{\{(ba)^2-(qa)^2\}^3} \\ S_{11} &= qa\left(\frac{1}{(ba)^2-(qa)^2} + \frac{4ba}{\{(ba)^2-(qa)^2\}^2} + \frac{2\{3(ba)^2+(qa)^2\}}{\{(ba)^2-(qa)^2\}^3}\right). \end{aligned} \tag{A.5}$$

For the inter-subband transition

$$\begin{aligned} G_{12}(q) &= \frac{(ba)^3\sqrt{3}}{2}\left(P_{12} + Q_{12} - \mathrm{e}^{-ba} f_{12}(q)\right) \\ P_{12} &= -\frac{8ba(qa)^2\{(ba)^2+(qa)^2\}}{\{(ba)^2-(qa)^2\}^4} \begin{Bmatrix} \cosh(qa/2) \\ -\sinh(qa/2) \end{Bmatrix} \\ Q_{12} &= -\frac{2qa\{(qa)^4+6(ba)^2(qa)^2+(ba)^4\}}{\{(ba)^2-(qa)^2\}^4} \begin{Bmatrix} -\sinh(qa/2) \\ \cosh(qa/2) \end{Bmatrix}. \end{aligned} \tag{A.6}$$

Once again the exponential term must be retained:

$$f_{12}(q) = \left(R_{11} - \frac{ba}{3}R_{12}\right)\begin{Bmatrix}\cosh(qa/2)\\ \sinh(qa/2)\end{Bmatrix} + \left(S_{11} - \frac{ba}{3}S_{12}\right)\begin{Bmatrix}\sinh(qa/2)\\ \cosh(qa/2)\end{Bmatrix}$$

$$R_{12} = \frac{ba}{(ba)^2-(qa)^2} + \frac{3\{(ba)^2+(qa)^2\}}{\{(ba)^2-(qa)^2\}^2} + \frac{6ba\{(ba)^2+3(qa)^2\}}{\{(ba)^2-(qa)^2\}^3} + \frac{6((ba)^4+6(ba)^2(qa)^2+(qa)^4)}{\{(ba)^2-(qa)^2\}^4} \tag{A.7}$$

$$S_{12} = qa\left(\frac{1}{(ba)^2-(qa)^2} + \frac{6ba}{\{(ba)^2-(qa)^2\}^2} + \frac{6\{3(ba)^2+(qa)^2\}}{\{(ba)^2-(qa)^2\}3} + \frac{24ba\{(ba)^2+(qa)^2\}}{\{(ba)^2-(qa)^2\}^4}\right).$$

3. Bulk modes

For the sake of completeness we give the well-known form factors for the Fang–Howard wavefunctions

$$F_{11}(q) = \frac{b}{8(q+b)^3}(8b^2+9bq+3q^2) \qquad F_{12}(q) = \frac{3bq}{16(q+b)^4}(5b^2+4bq+q^2). \tag{A.8}$$

The form factors for our model wavefunctions

$$\psi_1(z) = \left(\frac{b^5}{24}\right)^{1/2} z^2\,\mathrm{e}^{-bz/2} \qquad \psi_2(z) = \left(\frac{5b^5}{24}\right) z^2\left(1-\frac{bz}{5}\right)\mathrm{e}^{-bz/2} \tag{A.9}$$

are

$$F_{11}(q) = \frac{b}{128(b+q)^5}(128b^4+325b^3q+345b^2q^2+175bq^3+35q^4)$$
$$F_{12}(q) = \frac{5bq}{256(b+q)^6}(63b^4+122b^3q+102b^2q^2+42bq^3+7q^4). \tag{A.10}$$

References

[1] Fang F F and Howard W E 1966 *Phys. Rev. Lett.* **16** 797
[2] Fang F F and Howard W E 1967 *Phys. Rev.* **163** 816
[3] Nash K J, Skolnick M S and Bass S J 1987 *Semicond. Sci. Technol.* **2** 329
[4] Ridley B K 1999 *Phys. Status Solidi* a **176** 359
[5] Ridley B K, Zakhlenuik N A and Babiker M 2000 *Solid State Commun.* **116** 385
[6] Ridley B K 1992 *Proc. SPIE* **1675** 492
[7] Ridley B K 1993 *Phys. Rev.* B **47** 4592
[8] Constantinou N C and Ridley B K 1994 *Phys. Rev.* B **49** 17 065
[9] Camley R E and Mills D L 1984 *Phys. Rev.* B **29** 1695
[10] Herbert D C 1973 *J. Phys. C: Solid State Phys.* **6** 2788
[11] Mori N and Ando T 1989 *Phys. Rev.* B **40** 6175
[12] Nash K J 1992 *Phys. Rev.* B **46** 7723